

A quantum mechanical analysis of Smith-Purcell free-electron lasers

メタデータ	言語: eng 出版者: 公開日: 2017-10-03 キーワード (Ja): キーワード (En): 作成者: メールアドレス: 所属:
URL	http://hdl.handle.net/2297/42217

A quantum mechanical analysis of Smith-Purcell free-electron lasers

Hesham Fares^{1,2*} and Minoru Yamada^{1,3}

¹Faculty of Electrical and Computer Engineering, Institute of Science and Engineering,
Kanazawa University, Kakuma-machi, Kanazawa 920-1192, Japan.

²Department of Physics, Faculty of Science, Assiut University, Assiut 71516, Egypt.

³Department of Electronic System Engineering, Malaysia – Japan International Institute of
Technology (MJIT).

Abstract

The paper presents a quantum mechanical treatment for analyzing the Smith–Purcell radiation generated by charged particles passing over a periodic conducting structure. In our theoretical model, the electrons interact with a surface harmonic wave excited near the diffraction grating when the electron velocity is almost equal to the phase velocity of the surface wave. Then, the surface harmonic wave is electromagnetically coupled to a radiation mode. The dynamics of electrons is analyzed quantum mechanically where the electron is represented as a traveling electron wave with a finite spreading length. The conversion of the surface wave into a propagating mode is analyzed using the classical Maxwell's equations. In the small–signal gain regime, closed–form expressions for the contributions of the stimulated and spontaneous emissions to the evolution of the surface wave are derived. The inclusion of the spreading length of the electron wave to the emission spectral line is investigated. Finally, we compare our results based on the quantum mechanical description of electron and those based on the classical approach where a good agreement is confirmed.

*E-mail: fares_fares4@yahoo.com

1. Introduction

In 1953, S. J. Smith and E. M. Purcell firstly demonstrated that an optical light is emitted when an electron beam moves parallel and close over a metallic diffraction grating in vacuum [1]. The process was understood in terms of a simple model based on oscillations of the image charges induced on the metallic surface by electrons. The Smith–Purcell (SP) effect is widely considered as a possible mechanism for free–electron laser (FEL) operating over a wavelength range extending from the millimeter [2,3] to the optical region [4,5]. In recent experiments [6]–[8], it has been shown that the SP radiation provide a promising candidate to realize compact and tunable radiation source in the THz region. FELs based on the SP effect are operated in the amplifier and oscillator configurations where the optical feedback is required in the latter case [9]–[14]. Such FELs could be made with much more compact device structure compared to other FELs (e.g., undulator FELs), and therefore may be interesting for application.

Many theoretical analyses have been developed to analyze the dynamic of the Smith–Purcell radiation [15]–[22]. In most of these analyses, the metallic waveguide with periodic corrugation behaves as a slow wave structure through which a slow space harmonic of a transverse magnetic (TM) Floquet mode is propagated. The TM mode has a longitudinal electric field component and interacts most strongly with the traveling electrons. The working principle involves the synchronism between the velocity of the electron beam and the phase velocity of the TM surface modes of the periodic structure. The SP radiation contains a broad continuous frequency band and the radiation wavelength is determined by the observed angle, period of grating, and electron beam energy. Since the minimum corrugation period can be obtained currently is $\lesssim 0.1 \mu\text{m}$, the generation of SP radiation operating up to the ultraviolet is commonly accomplished by using nonrelativistic electron beams. In these cases, the radiation wavelength is a fraction of the corrugation period.

In all forgoing analyses, the interacting electron is consider as a point particle where its spreading size is assumed to be much shorter than the period of grating as well as the wavelength of emitted radiation. M. Yamada in [23] developed a quantum mechanical treatment for calculating the amplification gain of an optical amplifier in which an electron beam passes above a dielectric planer waveguide. This amplifier is basically one type of the Cherenkov FELs. The theoretical analysis was performed basing on the density matrix formalism which is a quantum statistical treatment [24]–[26]. In the theoretical model of [23,27,28], the electron is represented by an electron wave with a finite spreading length. In [27,28], the validity of the theoretical model is examined by comparing the experimentally measured data of intensities and spectrum profiles of optical radiation with those predicted theoretically. It is confirmed that the spectral profile of emission is characterized by the spreading length of the electron wave.

In this paper, we present a new theoretical analysis for the SP radiation in the small–signal

low gain regime. In our analysis, the dynamic of the EM wave is described using the Maxwell's wave equations. On the other hand, the dynamic of electrons are quantum mechanically analyzed using the density matrix formalism. We derive a generalized expression for the dispersion function that determines the spectral profile of emitted radiation. In this expression, the inclusion of the finite spreading length of the electron wave is studied. Our analysis is devoted for the nonrelativistic electron energies (≤ 100 keV). Also, since low-density beams are utilized in the SP experiments constructed to date, the space charge effects are neglected.

In Section 2, the analytical representations of the EM waves are shown. The EM wave is assumed to compose of surface modes that propagate along the corrugated surface and radiation modes that are emitted from the corrugated surface. Formulations of the radiation power and the stored energy are presented. In Section 3, the electron dynamics are described on the basis of the density matrix method. In Section 4, the gain coefficient of amplification by the stimulated emission and the radiation rate by the spontaneous emission are derived. In Section 5, the resonance condition for beam-radiation interaction is introduced, and that the spectrum characteristics of SP radiation are discussed in details. In Section 6, we present a comparison between our results and those obtained in a well-known classical analysis where a satisfactory agreement is reached. Finally, conclusions are given.

2. Analytical model and formulation of optical wave

2.1 Representation of optical wave

An illustration of the SP effect is shown in Fig. 1 where an electron beam moves at a distance h above a metallic corrugated surface with spatial periodicity Λ in the z direction. The depth direction of the corrugation is y and the width direction is x . The corrugation is uniform and oriented in the x direction. We also assume that that cross-sectional area of the electron beam is $w \times w$ in the $x - y$ plane.

Variations of the electric field $\mathbf{E}(x, y, z, t)$ and the magnetic field $\mathbf{H}(x, y, z, t)$ of the EM wave are given by Maxwell's wave equations as

$$\nabla^2 \mathbf{E} - \mu_0 \sigma(x, y, z) \frac{\partial \mathbf{E}}{\partial t} - \mu_0 \varepsilon(x, y, z) \frac{\partial^2 \mathbf{E}}{\partial t^2} = \mu_0 \frac{\partial \mathbf{J}}{\partial t}, \quad (1)$$

$$\nabla^2 \mathbf{H} - \mu_0 \sigma(x, y, z) \frac{\partial \mathbf{H}}{\partial t} - \mu_0 \varepsilon(x, y, z) \frac{\partial^2 \mathbf{H}}{\partial t^2} = -\nabla \times \mathbf{J}, \quad (2)$$

where $\sigma(x, y, z)$ and $\varepsilon(x, y, z)$ are the electrical conductivity and dielectric constant, respectively, which have different values in the metal and vacuum regions. $\mathbf{J}(x, y, z, t)$ is the current density of the electron beam where the moving electrons produces an EM wave on the grating. The interaction between the EM field localized close to the grating surface and the electron beam to obtain radiation power is counted through this current density \mathbf{J} . The evaluation of \mathbf{J} is performed with the help of quantum mechanical treatment assuming the electron wave

representation as will be given in following sections. In our model, it is assumed that a sufficiently intense magnetostatic field in the direction of the beam flow is applied. Then, the electron beam is considered to be thin where the transverse velocities of electrons in the direction normal to the electrons propagation can be neglected. In the limit of a thin electron beam, we can neglect the effects of the self-magnetic fields in the transverse directions on the longitudinal modulations of electrons. Therefore, the EM wave is restricted to be a TM mode having H_x , E_y and E_z components where the z -component of the electric field E_z interacts most strongly with the electrons.

We define the spatial wavenumber of the corrugation corresponding to the grating period Λ as

$$G = \frac{2\pi}{\Lambda}, \quad (3)$$

Here, we assume the position of the metal surface in the vertical direction y is varied as

$$y_0 = \sum_{m \geq 0} d_m \cos(mGz) = \sum_{m \geq 0} \frac{d_m}{2} (e^{jmGz} + e^{-jmGz}). \quad (4)$$

In Eq. (4), m is an integer and the Fourier coefficients d_m determine the peak-to-peak depth of the grating whereas d_0 refers to the average depth of the periodic structure. As shown in Fig. 1, we set $y = 0$ at the top boundary of the corrugation, the interaction length is L_z , and the distribution width of the EM wave is L_x . A part of the energy associated with the surface waves is transformed as radiation waves. The wavenumbers of both types of waves along z direction are modified by the corrugation, and then the fields' distribution is critically modified by the corrugation.

The magnetic field component H_x can be written as

$$H_x(x, y, z, t) = H_r(x, y, z, t) + H_s(x, y, z, t). \quad (5)$$

In Eq. (5), H_r is a radiation wave component and is given by

$$H_r = \tilde{E}(t) \sqrt{\frac{\epsilon_0}{\mu_0}} \{R^{(+)} e^{-j\gamma y - j\beta z} + R^{(-)} e^{-j\gamma y + j\beta z}\} e^{j\omega t} + c. c., \quad (6)$$

and H_s is a surface field expressed as a superposition of plane waves of different frequencies as

$$H_s = \tilde{E}(t) \sqrt{\frac{\epsilon_0}{\mu_0}} U_x(x, y, z) e^{j\omega t} + c. c., \quad (7)$$

where

$$U_x(x, y, z) = \sum_{m=-\infty}^{m=\infty} \{A_m^{(+)}(y, z) e^{-j(mG+\beta)z} + A_m^{(-)}(y, z) e^{-j(mG-\beta)z}\}. \quad (8)$$

Here, ω is the angular frequency, $\tilde{E}(t)$ is the temporal field amplitude and $c. c.$ indicates the complex conjugate of the preceding terms. β and γ are the wavenumbers (i.e., propagation constants) in the z and y directions of the radiation wave, respectively. Superscripts (+) and (-) indicate the forward and backward propagating components along z direction, respectively.

$R^{(\pm)}$ and $A_m^{(\pm)}$ are amplitude coefficients and amplitude functions, respectively.

The radiation field H_r exists only in the vacuum region where $y \geq 0$. By putting $\varepsilon = \varepsilon_0$, $\sigma = 0$, and $\mathbf{J} = 0$ in Eq. (2), the relation between wavenumbers is

$$\beta^2 + \gamma^2 = \mu_0 \varepsilon_0 \omega^2 = \frac{\omega^2}{c^2}. \quad (9)$$

The amplitude functions of the surface wave $A_m^{(\pm)}(y, z)$ are assumed to be varied much slower than the spatial phase variation in the z direction $e^{-j(mG \pm \beta)z}$. Then, the surface wave must be an evanescent wave for $\pm y$ direction where $|mG \pm \beta| > \omega/c$, and satisfies the relation of

$$A_m^{(\pm)}(y, z) \rightarrow 0 \quad \text{for } |y| \rightarrow \infty \text{ and } m \neq 0. \quad (10)$$

The principle surface mode (i.e., $m = 0$) having the amplitude $A_0^{(\pm)}(y, z)$ is rather exceptional. This mode directly couples to the radiation wave at $y = 0$, because this term has identical propagation constant $\pm\beta$ along z direction. Hence, we can write

$$A_0^{(\pm)}(y, z) = 0 \quad \text{for } y > 0, \quad (11 - a)$$

$$A_0^{(\pm)}(y, z) = R^{(\pm)} \quad \text{for } y = 0, \quad (11 - b)$$

$$|A_0^{(\pm)}(y, z)| \rightarrow 0 \quad \text{for } y \rightarrow -\infty, \quad (11 - c)$$

By separating the EM wave into radiation and surface waves, we also represent the electric field component \mathbf{E} as

$$\mathbf{E}(x, y, z, t) = \mathbf{E}_r(x, y, z, t) + \mathbf{E}_s(x, y, z, t), \quad (12)$$

where \mathbf{E}_r and \mathbf{E}_s are the radiation and surface field components, respectively, and are given by

$$\mathbf{E}_r = \tilde{E}(t) \mathbf{Q}(x, y, z) e^{j\omega t} + c. c., \quad (13)$$

$$\mathbf{E}_s = \tilde{E}(t) \mathbf{F}(x, y, z) e^{j\omega t} + c. c., \quad (14)$$

$\mathbf{Q}(x, y, z)$ and $\mathbf{F}(x, y, z)$ are field distribution functions and are derived from the magnetic component H_x using the relations of $E_y = \{1/(j\omega\varepsilon + \sigma)\}(\partial H_x/\partial z)$ and $E_z = \{-1/(j\omega\varepsilon + \sigma)\}(\partial H_x/\partial y)$, resulting in

$$Q_y(x, y, z) = \frac{c\beta}{\omega} \{-R^{(+)} e^{-j\gamma y - j\beta z} + R^{(-)} e^{-j\gamma y + j\beta z}\}, \quad (15)$$

$$Q_z(x, y, z) = \frac{c\gamma}{\omega} \{R^{(+)} e^{-j\gamma y - j\beta z} + R^{(-)} e^{-j\gamma y + j\beta z}\}, \quad (16)$$

$$F_y(x, y, z) = \frac{-1}{(\omega\varepsilon - j\sigma)} \sqrt{\frac{\varepsilon_0}{\mu_0}} \sum_{m=-\infty}^{m=\infty} \{(mG + \beta) A_m^{(+)}(y, z) e^{-j(mG + \beta)z} + (mG - \beta) A_m^{(-)}(y, z) e^{-j(mG - \beta)z}\}, \quad (17)$$

$$F_z(x, y, z) = \frac{j}{(\omega\varepsilon - j\sigma)} \sqrt{\frac{\varepsilon_0}{\mu_0}} \sum_{m=-\infty}^{m=\infty} \left\{ \frac{\partial A_m^{(+)}(y, z)}{\partial y} e^{-j(mG + \beta)z} + \frac{\partial A_m^{(-)}(y, z)}{\partial y} e^{-j(mG - \beta)z} \right\}, \quad (18)$$

In the vacuum region where $y > 0$, the amplitude functions must be given by

$$A_m^{(\pm)}(y, z) = A_m^{(\pm)}(0, z)e^{-\gamma_m^{(\pm)}y} \text{ for } y > 0, \quad (19)$$

with the relation of

$$(mG \pm \beta)^2 - \gamma_m^{(\pm)2} = \frac{\omega^2}{c^2}, \quad (20)$$

Therefore, the distribution functions are given by

$$F_y(x, y, z) = -\frac{c}{\omega} \sum_{m=-\infty}^{m=\infty} \left\{ (mG + \beta) A_m^{(+)}(0, z) e^{-\gamma_m^{(+)}y - j(mG + \beta)z} + (mG - \beta) A_m^{(-)}(0, z) e^{-\gamma_m^{(-)}y - j(mG - \beta)z} \right\} \\ , \text{ for } y > 0 \quad (21)$$

$$F_z(x, y, z) = -j \frac{c}{\omega} \sum_{m=-\infty}^{m=\infty} \left\{ \gamma_m^{(+)} A_m^{(+)}(0, z) e^{-\gamma_m^{(+)}y - j(mG + \beta)z} + \gamma_m^{(-)} A_m^{(-)}(0, z) e^{-\gamma_m^{(-)}y - j(mG - \beta)z} \right\} \\ , \text{ for } y > 0 \quad (22)$$

2.2 Condition of the Smith–Purcell radiation

Here, we examine the SP radiation condition basing on our notation. Assuming the radiation angle is θ as shown in Fig. 1, we get

$$\pm\beta = \frac{\omega}{c} \cos(\theta), \quad (23)$$

$$\gamma = \frac{\omega}{c} \sin(\theta), \quad (24)$$

where $+\beta$ and $-\beta$ correspond to the cases of forward and backward propagations when $0 \leq \theta \leq \pi/2$ and $\pi/2 \leq \theta \leq \pi$, respectively.

To generate the SP radiation, the velocity of electron v_e must coincide with the phase velocity of the induced wave, that is

$$(mG \pm \beta)v_e = \omega, \quad (25)$$

By substituting Eq. (23) into Eq. (25), we get the relation of

$$\omega = \frac{2m\pi c}{\Lambda} \left\{ \frac{1}{\left[\frac{c}{v_e} - \cos(\theta) \right]} \right\}. \quad (26)$$

Equation (26) can be rewritten in terms of the emitted wavelength as

$$\lambda = \frac{\Lambda}{m} \left[\frac{c}{v_e} - \cos(\theta) \right]. \quad (27)$$

which is the well-known resonance condition of the SP radiation.

The relation between the angular frequency and the EM wavenumber along z direction is illustrated in Fig. 2. The lines $\omega = \pm c\beta$ correspond to the case of $\gamma = 0$ at which $\theta = 0$. When the operating point is located between the light lines (i.e., $\omega = \pm c\beta$), the radiation into vacuum space is generated. The beam line $\omega = (mG \pm \beta)v_e$ indicates the condition of the interaction between the EM field and the electron beam. If the interaction is occurred at a point P , other

operating points P' , P'' , $P''' \dots$ given with different number of m , are also induced. Then the radiation is generated at the point P'' in Fig. 2.

A schematic illustration of the analytic model used in this paper is described in Fig. 3. The electron beam interacts with one field harmonic having the modified wavenumber of $mG \pm \beta$. This interaction will be analyzed in Sec. II basing on the density matrix method. Although the EM wave is separated into different modes, but they are coupled to each other, and then the radiation wave is generated. This coupling is explained by the Maxwell's wave equation.

2.3 Radiating power and stored energy

The Poynting vector of the radiating wave for θ or $\pi - \theta$ direction is

$$|\mathbf{E}_r^{(\pm)} \times \mathbf{H}_x^{(\pm)}| = 2 \sqrt{\frac{\varepsilon_0}{\mu_0}} |R^{(\pm)}|^2 |\tilde{E}(t)|^2 \sin(\theta). \quad (28)$$

Then, the total radiation power P emitted from the corrugated surface is

$$\begin{aligned} P &= \int_0^{L_y} \int_0^{L_x} \left\{ \mathbf{E}_r^{(+)} \times \mathbf{H}_x^{(+)} + \mathbf{E}_r^{(-)} \times \mathbf{H}_x^{(-)} \right\} \sin(\theta) dx dy \\ &= 2L_x L_y \sin(\theta) \sqrt{\frac{\varepsilon_0}{\mu_0}} \left\{ |R^{(+)}|^2 + |R^{(-)}|^2 \right\} |\tilde{E}(t)|^2. \end{aligned} \quad (29)$$

Here, we define the normalization of the electric field components of the surface wave as

$$\begin{aligned} \int_0^{L_z} \int_{-\infty}^{\infty} \int_0^{L_x} |\mathbf{F}(x, y, z)|^2 dx dy dz &= \int_0^{L_z} \int_{-\infty}^{\infty} \int_0^{L_x} \left\{ |F_y(x, y, z)|^2 + |F_z(x, y, z)|^2 \right\} dx dy dz \\ &= \frac{\varepsilon_0}{\mu_0} \int_0^{L_z} \int_{-\infty}^{\infty} \int_0^{L_x} \left[\frac{1}{(\omega\varepsilon)^2 + \sigma^2} \sum_{m=-\infty}^{m=\infty} \left\{ (mG + \beta)^2 |A_m^{(+)}|^2 + \left| \frac{\partial A_m^{(+)}}{\partial y} \right|^2 + (mG - \beta)^2 |A_m^{(-)}|^2 \right. \right. \\ &\quad \left. \left. + \left| \frac{\partial A_m^{(-)}}{\partial y} \right|^2 \right\} \right] dx dy dz = 1. \end{aligned} \quad (30)$$

The stored energy of the surface wave is

$$\begin{aligned} W &= \frac{1}{2} \int_0^{L_z} \int_{-\infty}^{\infty} \int_0^{L_x} [\varepsilon \mathbf{E}_s^2 + \mu_0 \mathbf{H}_s^2] dx dy dz \\ &= \left[\varepsilon_{av} + \varepsilon_0 \int_0^{L_z} \int_{-\infty}^{\infty} \int_0^{L_x} \sum_{m=-\infty}^{m=\infty} \left\{ |A_m^{(+)}(y, z)|^2 + |A_m^{(-)}(y, z)|^2 \right\} dx dy dz \right] |\tilde{E}(t)|^2. \end{aligned} \quad (31)$$

where

$$\varepsilon_{av} = \int_0^{L_z} \int_{-\infty}^{\infty} \int_0^{L_x} \varepsilon |\mathbf{F}(x, y, z)|^2 dx dy dz. \quad (32)$$

is an averaged dielectric constant for the surface wave.

2.4 Equation for evolution of the EM wave

The surface evanescent wave loses energy due to the transformation into radiation and the

unavoidable loss of metallic grating. Therefore, we define a decay time τ_{rad} as an eigen value of the following equation

$$\left\{ \nabla^2 - \mu_0 \sigma(x, y, z) \frac{\partial}{\partial t} - \mu_0 \varepsilon(x, y, z) \frac{\partial^2}{\partial t^2} \right\} \mathbf{F}(x, y, z) e^{(j\omega - \frac{1}{2\tau_{rad}})t} = 0. \quad (33)$$

Assuming $\omega \gg 1/\tau_{rad}$, we get from Eq. (33)

$$\{ \nabla^2 - j\omega\mu_0 \sigma + \omega^2\mu_0\varepsilon \} \mathbf{F}(x, y, z) = -\frac{\mu_0}{\tau_{rad}} \left(\frac{\sigma}{2} + j\omega \varepsilon \right) \mathbf{F}(x, y, z). \quad (34)$$

By substituting Eqs. (12)–(14) into Eq. (1), using the relations of Eqs. (9) and (34), and neglecting the second derivative of $\tilde{E}(t)$ (i. e., $\partial^2 \tilde{E}/\partial t^2 \approx 0$), we get the following equation

$$-\left\{ 2j\omega\varepsilon_0 \frac{\partial \tilde{E}}{\partial t} \mathbf{Q} + (\sigma + 2j\omega\varepsilon) \frac{\partial \tilde{E}}{\partial t} \mathbf{F} + \frac{1}{\tau_{opt}} \left(\frac{\sigma}{2} + j\omega\varepsilon \right) \tilde{E} \mathbf{F} \right\} e^{j\omega t} + c. c. = \frac{\partial \mathbf{J}}{\partial t}, \quad (35)$$

By multiplying both sides of Eq. (35) by $\mathbf{F}^* e^{-j\omega t}$, taking the spatial integration in the defined space, and using the relation of $\partial \mathbf{J}/\partial t = j\omega \mathbf{J} = j\omega \mathbf{J} \vec{\mathbf{k}}$ where $\vec{\mathbf{k}}$ is the unit vector in the z direction, we get

$$\frac{d\tilde{E}}{dt} = -\frac{1}{2\varepsilon_{av}} \int_0^{L_z} \int_h^{w+h} \int_{-w/2}^{w/2} \langle \mathbf{J} \mathbf{F}_z^* e^{-j\omega t} \rangle dx dy dz - \frac{\tilde{E}(t)}{2\tau_{rad}}, \quad (36)$$

with

$$\varepsilon_{av} = \int_0^{L_z} \int_{-\infty}^{\infty} \int_{-w/2}^{w/2} \left(\varepsilon - j \frac{\sigma}{2\omega} \right) |\mathbf{F}(x, y, z)|^2 dx dy dz. \quad (37)$$

In Eq. (36), $\langle \rangle$ refers to the operation of the quantum statistical average.

To get a sufficient gain for laser oscillation, the radiating power should be larger than the power lost by the grating absorption, and hence, we approximately write

$$\frac{1}{\tau_{rad}} \approx \frac{P}{W}, \quad (38)$$

where P is the total radiation power given by Eq. (29) and W is the stored energy of the surface wave as given in Eq. (32)

3. Electron dynamics

From the SP condition shown in Eq. (27), the radiated wavelength λ can be reduced by decreasing the corrugation period Λ . The metallic corrugation assists in establishing the phase variation of the EM field. It is noticed that the corrugated metallic surface behaves as the static magnetic field in the undulator FEL. As SP experiments move toward the generation of shorter wavelength radiation, shorter corrugation periods are required. The minimum Λ obtained currently can be in the order of few tenths of micrometers. When the corrugation period becomes shorter than the spreading length of an electron wave, which is in the order of tens of micrometers ($\sim 40 \mu\text{m}$) [27,28], the electron sees non-uniform dielectric constant along a single electron. Equivalently, an electron wave is subjected to a spatially variant electric force from the surface EM wave. In this paper, we take into account the quantum mechanical representation of

an electron. Then we examine the validity of the quantum model by examining the operating conditions at which this model reveals similar results of the classical treatments.

By assigning a number ν for each electron in the electron beam, the electron wave function is given by

$$\Psi(t, \mathbf{r}) = \sum_f c_f^{(\nu)}(t) \phi_f(\mathbf{r}) e^{-j\omega_f t}. \quad (39)$$

where $\phi_f(\mathbf{r})$ is a spatial distribution function of an electron wave at the f – th energy state.

The coefficient $c_f^{(\nu)}(t)$ weights the contribution of the f – th energy state to the ν – th electron.

In the quantum mechanical framework, an electron must be considered as a wave packet with a finite length. The electron packet can be expressed in the form of linear superposition of plane waves. Since the summation over all possible wavenumbers is inherent in calculating the expectation values, it is mathematically favorable to express the electron wave function in the form of a plane wave. In this work, we use the formulation of the electron wave as introduced in Ref. [29], where the electron wave is assumed to be a plane wave which spreads in a rectangular box whose volume is ℓ^3

$$|f\rangle = \phi_f(\mathbf{r}) = \frac{1}{\ell^{3/2}} e^{jk_f z}. \quad (40)$$

Equations (39) and (40) state that the electron travels in the form of $\exp[j(k_f z - \omega_f t)]$. In Ref. [29], it is shown that the representation of the electron wave as a plane wave simplifies the calculation of the coupling between the electron wave and EM wave.

The density matrix formalism is a quantum statistical method and is suitable to obtain the expectation value of the beam dynamic coefficients such as $\langle JF_z^* e^{-j\omega t} \rangle$ shown in Eq. (36). The basic formulations of the density matrix method are reviewed in the Appendix of this paper. Further discussions on the density matrix can be found in Ref. [30]. The expectation value of an arbitral operator or function $\langle \mathbf{R} \rangle$ is obtained by (i.e., see Eq. (A8) in the Appendix)

$$\langle \mathbf{R} \rangle = \sum_{g \neq f} \sum_f \rho_{fg}(t) \mathcal{R}_{gf} = \sum_f \langle f | \rho \mathbf{R} | f \rangle = \text{Tr}(\rho \mathbf{R}), \quad (41)$$

where $\text{Tr}(\dots)$ is the trace operation, ρ is the density matrix in which the dynamic of an electron is involved, and $|f\rangle$ is an eigen state of an electron. By introducing the identity operator

$$I = \sum_g |g\rangle \langle g|, \quad (42)$$

the first term in the right–hand side of Eq. (36) is given as

$$\langle JF_z^* e^{-j\omega t} \rangle = \sum_f \sum_g \langle f | \rho | g \rangle \langle g | JF_z^* e^{-j\omega t} | f \rangle, \quad (43)$$

As shown in Eq. (A12), the dynamics of an electron are described using the dynamic equation of the density matrix

$$\frac{d\rho}{dt} = \frac{1}{j\hbar} [(H_0 + H_{\text{int}}), \rho] - \frac{1}{2} \{(\rho - \tilde{\rho})\Gamma + \Gamma(\rho - \tilde{\rho})\}, \quad (44)$$

where H_0 and H_{int} are the principal “free” and interaction Hamiltonians of electrons, respectively. $\tilde{\rho}$ is a distribution function of electrons at the thermal equilibrium. Γ is an operator representing the relaxation effect of the electron wave due to the mutual scattering of electrons.

In Eq. (44), the principal Hamiltonian H_0 has the property of

$$\langle f|H_0|g\rangle = W_f\delta_{f,g}, \quad (45)$$

where

$$W_f = \frac{\hbar^2 k_f^2}{2m_0} = \frac{m_0 v_f^2}{2} = \hbar\omega_f. \quad (46)$$

H_{int} is given by

$$H_{\text{int}} = j \frac{e}{2m_0\omega} (pE_z + E_z p) + H.c., \quad (47)$$

where e is the electron charge unit, m_0 is the rest mass of an electron, E_z is the z component of the electric field, p is the momentum operator, and $H.c.$ means the Hermite conjugate of the preceding terms. Γ is assumed to have only diagonal elements and whose expectation value is $1/\tau_e$, where τ_e is the electron relaxation time,

$$\langle f|\Gamma|g\rangle = 1/\tau_e\delta_{f,g}. \quad (48)$$

In our study, for weakly pumped SP FELs operated in the low gain regime (i.e., the electron beam current is below 1 A), we neglect the space–charge (collective) effects. At high electron densities, the inclusions of the space–charge effects can be considered by taking into account the static electric field of neighboring electrons in the dynamics formulations. This can be done by considering the scalar potential U , generated by the surrounding modulated electrons, in the electron Hamiltonian given by Eq. (47) (i.e., the term $-eU$ appears as an additional term on the left–hand side of Eq. (47)). Detailed discussions on how to take into count the space charge effects can be found in Refs. [25,31].

The electron current density \mathbf{J} is given in terms of the electron density N and the quantum mechanical operator of p (or v),

$$\mathbf{J} = -eN\mathbf{v} = -\frac{eN}{m_0}\mathbf{p}. \quad (49)$$

Since the momentum operator p has diagonal elements only where

$$\langle f|p|g\rangle = \hbar k_f\delta_{f,g} = m_0 v_f\delta_{f,g}, \quad (50)$$

the expectation value of $\langle \mathbf{J}F_z^* e^{-j\omega t} \rangle$ in Eq. (43) can be rewritten as

$$\langle \mathbf{J}F_z^*(x, y, z)e^{-j\omega t} \rangle = -\sum_f \sum_g e\bar{N}v_g \langle f|\rho|g\rangle \langle g|F_z^*(x, y, z)|f\rangle e^{-j\omega t}, \quad (51)$$

where \bar{N} is the spatially averaged electron density in the electron beam. From Eq. (A7), the diagonal element of the density matrix $\rho_{ff}(t) = \sum_v P^{(v)} |c_f^{(v)}(t)|^2$ represents the total probability of finding the electron in a specific state $|\phi_f\rangle$. The off–diagonal element of the density

matrix $\rho_{fg}(t)$ corresponds to the transition state of an electron where the electron transits from level f to level g (i.e., the mixed state). In the time interval of the electron transition, the electron wave has a beating vibration of $e^{-j(\omega_f - \omega_g)t}$. Note that $\rho_{fg}(t)$ is also proportional to $e^{-j(\omega_f - \omega_g)t}$ as shown in Eq. (A7). When this beating vibration coincides with the phase vibration of the EM wave $e^{-j\omega t}$ (i.e., $\omega_f - \omega_g = \omega$) corresponding to the energy conservation rule, the interaction occurs. From the above discussion, the electron density can be treated as a quantum mechanical operator in the form of $\bar{N}\rho$. For the double summations over energy levels f and g in Eq. (51), the case of $f = g$ represents a dynamic motion of an electron without making any transition from the initial energy level f to other energy levels. In this case, the term $\bar{N}\langle f|\rho|f\rangle = \bar{N}\rho_{ff}$ in Eq. (51) denotes the average component of the electron density (or the average current density). In the case of $f \neq g$ in the double summations of Eq. (51), the term $\bar{N}\langle f|\rho|g\rangle = \bar{N}\rho_{fg}$ denotes the modulated component of the electron density (or the modulated term current density).

By substituting Eqs. (45)–(48) into Eq. (44), the dynamic equation for the off-diagonal element of the density matrix ρ_{fg} is given by

$$\frac{d\rho_{fg}}{dt} = -j\omega_{fg}\rho_{fg} + \frac{e}{2m_0\hbar\omega} \{ \langle f|pE_z\rho|g\rangle + \langle f|E_zp\rho|g\rangle - \langle f|\rho pE_z|g\rangle - \langle f|\rho E_zp|g\rangle \} - \frac{\rho_{fg}}{\tau_e}, \quad (52)$$

In Eq. (52),

$$\langle f|pE_z\rho|g\rangle = m_0v_f\langle f|E_z|g\rangle\rho_{gg}, \quad (53)$$

$$\langle f|E_zp\rho|g\rangle = \langle f|E_z|g\rangle m_0v_g\rho_{gg}, \quad (54)$$

$$\langle f|\rho pE_z|g\rangle = \rho_{ff}m_0v_f\langle f|E_z|g\rangle, \quad (55)$$

$$\langle f|\rho E_zp|g\rangle = \rho_{ff}\langle f|E_z|g\rangle m_0v_g, \quad (56)$$

For the electric field interacting with the electron beam and is given by Eqs. (12), (14) and (22), we define the off-diagonal element of the field distribution of the surface wave $F_z(x, y, z)$ as

$$\langle f|F_z(x, y, z)|g\rangle = \sum_{m=-\infty}^{m=\infty} [F_{mfg}^{(+)} + F_{mfg}^{(-)}], \quad (57)$$

with

$$F_{mfg}^{(\pm)} = -\frac{j\gamma_m^{(\pm)}A_m^{(\pm)}(0, z)}{\omega} \langle f|e^{-\gamma_m^{(\pm)}y - j(mG \pm \beta)z}|g\rangle. \quad (58)$$

Using Eq. (40) of the electron wave function, the inner product in Eq. (58) will be

$$\langle f|e^{-\gamma_m^{(\pm)}y - j(mG \pm \beta)z}|g\rangle = \frac{1}{\ell^3} \int_0^\ell \int_0^\ell \int_0^\ell e^{-\gamma_m^{(\pm)}y - j(k_g - k_f - mG \pm \beta)z} dx dy dz. \quad (59)$$

Hence, Eq. (58) becomes

$$F_{mfg}^{(\pm)} = -\frac{j\gamma_m^{(\pm)}A_m^{(\pm)}(0, z)}{\omega} \left(\frac{1 - e^{-\gamma_m^{(\pm)}\ell}}{\gamma_m^{(\pm)}\ell} \right) e^{j(k_g - k_f - mG \mp \beta)\ell/2} \times \text{Sinc}\{(k_g - k_f - mG \mp \beta)\ell/2\}. \quad (60)$$

where $\text{Sinc}(X) = \sin(X)/X$. From Eq. (60), it is shown that $F_{mfg}^{(\pm)}$ becomes maximum when

$k_g - k_f - mG \mp \beta = 0$ which implies the momentum conservation rule for the electron transition. This transition is caused by the coupling between the electron and EM waves for a specific geometry of metallic corrugation.

Another inner product for the complex conjugate of the field distribution function is

$$\langle f|F_z^*(x, y, z)|g\rangle = \langle g|F_z(x, y, z)|f\rangle^* = \sum_{m=-\infty}^{m=\infty} [F_{mfg}^{(+)*} + F_{mfg}^{(-)*}], \quad (61)$$

Using Eqs. (57) and (61), we obtain

$$\langle f|E_z|g\rangle = \tilde{E}(t) \sum_{m=-\infty}^{m=\infty} [F_{mfg}^{(+)} + F_{mfg}^{(-)}] e^{j\omega t} + \tilde{E}^*(t) \sum_{m=-\infty}^{m=\infty} [F_{mfg}^{(+)*} + F_{mfg}^{(-)*}] e^{-j\omega t}. \quad (62)$$

Then the dynamic equation depicted by Eq. (52) is rewritten as

$$\begin{aligned} \frac{d\rho_{fg}}{dt} &= -j\omega_{fg}\rho_{fg} \\ &+ \frac{e(v_f + v_g)(\rho_{gg} - \rho_{ff})}{2\hbar\omega} \left\{ \tilde{E}(t) \sum_{m=-\infty}^{m=\infty} [F_{mfg}^{(+)} + F_{mfg}^{(-)}] e^{j\omega t} \right. \\ &\left. + \tilde{E}^*(t) \sum_{m=-\infty}^{m=\infty} [F_{mfg}^{(+)*} + F_{mfg}^{(-)*}] e^{-j\omega t} \right\} - \frac{\rho_{fg}}{\tau_e}, \end{aligned} \quad (63)$$

The solution of Eq. (63) takes the form

$$\begin{aligned} \rho_{fg} &= \frac{e(v_f + v_g)(\rho_{gg} - \rho_{ff})}{2\hbar\omega} \left\{ \frac{\tilde{E}(t)}{j(\omega - \omega_{gf}) + \frac{1}{\tau_e}} \sum_{m=-\infty}^{m=\infty} [F_{mfg}^{(+)} + F_{mfg}^{(-)}] \left[e^{j\omega t} - e^{(j\omega_{gf} - \frac{1}{\tau_e})t} \right] \right. \\ &\left. + \frac{\tilde{E}^*(t)}{-j(\omega + \omega_{gf}) + \frac{1}{\tau_e}} \sum_{m=-\infty}^{m=\infty} [F_{mfg}^{(+)*} + F_{mfg}^{(-)*}] \left[e^{-j\omega t} - e^{(j\omega_{gf} - \frac{1}{\tau_e})t} \right] \right\}, \end{aligned} \quad (64)$$

Using Eq. (64), Eq. (43) becomes

$$\begin{aligned} \langle JF_z^*(x, y, z)e^{-j\omega t} \rangle &= \\ &- \sum_{g>f} \sum_f \sum_{m=0} \frac{e^2 \bar{N} v_g (v_f + v_g) (\rho_{gg} - \rho_{ff})}{2\hbar\omega \left[j(\omega - \omega_{gf}) + \frac{1}{\tau_e} \right]} \left\{ \sum_{m=-\infty}^{m=\infty} \left[|F_{mfg}^{(+)}|^2 + |F_{mfg}^{(-)}|^2 \right] \left[1 - e^{[j(\omega_{gf} - \omega) - \frac{1}{\tau_e}]t} \right] \right\} \tilde{E}(t), \end{aligned} \quad (65)$$

4. Radiation gain and spontaneous emission

By substituting Eq. (65) into Eq. (36), we get the following equation for the temporal variation of the field amplitude

$$\begin{aligned} \frac{d\tilde{E}}{dt} &= \int_0^{L_z} \int_h^{w+h} \int_{-w/2}^{w/2} \sum_{g>f} \sum_f \sum_{m=0} \frac{e^2 \bar{N} v_g (v_f + v_g) (\rho_{gg} - \rho_{ff})}{4\hbar\omega \tilde{\epsilon}_{av} \left[j(\omega - \omega_{gf}) + \frac{1}{\tau_e} \right]} \left\{ \sum_{m=-\infty}^{m=\infty} \left[|F_{mfg}^{(+)}|^2 + |F_{mfg}^{(-)}|^2 \right] \right\} dx dy dz \\ &\times \left[1 - e^{[j(\omega_{gf} - \omega) - \frac{1}{\tau_e}]t} \right] \tilde{E}(t) - \frac{\tilde{E}(t)}{2\tau_{rad}}, \end{aligned}$$

(66)

From Eq. (66), the variation of the EM wave intensity is given by

$$\frac{d|\tilde{E}(t)|^2}{dt} = \frac{d\tilde{E}(t)}{dt} \tilde{E}^*(t) + \frac{d\tilde{E}^*(t)}{dt} \tilde{E}(t) = \left(G_{st} - \frac{1}{\tau_{rad}} \right) |\tilde{E}(t)|^2, \quad (67)$$

where G_{st} is the gain coefficient given by

$$G_{st} = \int_0^{L_z} \int_h^{w+h} \int_{-w/2}^{w/2} \sum_{g>f} \sum_f \sum_{m=0} \frac{e^2 \bar{N} v_g (v_f + v_g) (\rho_{gg} - \rho_{ff})}{4 \hbar \omega \tilde{\epsilon}_{av} \left[j(\omega - \omega_{gf}) + \frac{1}{\tau_e} \right]} \left\{ \sum_{m=-\infty}^{m=\infty} \left[|F_{mfg}^{(+)}|^2 + |F_{mfg}^{(-)}|^2 \right] \right\} dx dy dz \\ \times \left[1 - e^{\left[j(\omega_{gf} - \omega) - \frac{1}{\tau_e} \right] t} \right], \quad (68)$$

with

$$|F_{mfg}^{(\pm)}|^2 = \left\{ \frac{c}{\omega} \left(\frac{1 - e^{-\gamma_m^{(\pm)} \ell}}{\ell} \right) \right\}^2 |A_m^{(\pm)}(0, z)|^2 \text{Sinc}^2\{(k_g - k_f - mG \mp \beta)\ell/2\}. \quad (69)$$

Assuming that the initial energy level of electron is b where it transits to a lower energy level a resulting in an emission and transits to a higher energy level c resulting in absorption. The emission and absorption process satisfy the relations of

$$\omega_b - \omega_a = \omega, \quad (70)$$

and

$$\omega_c - \omega_b = \omega, \quad (71)$$

with the condition of

$$\rho_{aa} = \rho_{cc} = 0, \quad (72)$$

Eq. (72) state that the there is a zero probability of finding an electron at final energy levels a and c assuming the energy separation of $\hbar\omega$ is much larger than the thermal energy of the electron beam.

Using Eqs. (70)–(72), the gain coefficient shown in Eq. (68) becomes

$$G_{st} = \int_0^{L_z} \int_h^{w+h} \int_{-w/2}^{w/2} \sum_b \sum_{m=0} \frac{e^2 \bar{N} v_b^2 \rho_{bb} \tau_e}{\tilde{\epsilon}_{av} \hbar \omega} \left\{ \sum_{m=-\infty}^{m=\infty} \left[|F_{mab}^{(+)}|^2 + |F_{mab}^{(-)}|^2 - |F_{mbc}^{(+)}|^2 - |F_{mbc}^{(-)}|^2 \right] \right\} dx dy dz \\ \times \left[1 - e^{-\frac{t}{\tau_e}} \right], \quad (73)$$

The average current density \bar{J} can be represented in terms of the diagonal element ρ_{bb} and the initial electron velocity $v_e = v_b$ as

$$\bar{J} = e \langle N v \rangle = e \sum_b \bar{N} v_b \rho_{bb} = e \bar{N} v_e, \quad (74)$$

Here, it is instructive to point that a forward/or/backward component with a specific m can satisfy the condition $k_g - k_f - mG \mp \beta \approx 0$ according to the momentum conservation rule. The radiation wave can never interact with the electron beam in the absence of the corrugation since $k_g - k_f \mp \beta \neq 0$.

We define a spatial coupling coefficient ξ_m as

$$\xi_m = L_z \int_h^{w+h} \int_{-w/2}^{w/2} \left\{ \frac{c}{\omega} \left(\frac{1 - e^{-\gamma_m^{(\pm)} \ell}}{\ell} \right) \right\}^2 |A_m^{(\pm)}|^2 dx dy. \quad (75)$$

and a dispersion function D_{stm} as

$$D_{stm} = \text{Sinc}^2\{(k_b - k_a - mG \mp \beta)\ell/2\} - \text{Sinc}^2\{(k_c - k_b - mG \mp \beta)\ell/2\}. \quad (76)$$

Since our model is restricted to the low gain regime of SP FELs, we can neglect the variations in the refractive indices of the electron beam and metal regions due to the presence of the electron beam. In this limit, to evaluate the coupling coefficient ξ_m given in Eq. (75), possible solutions for the amplitude functions of the surface wave $A_m^{(\pm)}$ can be found in [32].

Combining Eqs. (74)–(76) with Eq. (73), the gain coefficient is rewritten in a simple form as

$$G_{st} = \frac{e\bar{j}v_e\tau_e \left[1 - e^{-\frac{t}{\tau_e}} \right]}{\bar{\epsilon}_{av}\hbar\omega} \xi_m D_{stm}. \quad (77)$$

In Eq. (77), t is considered as the interaction time counted as the time interval for passing the interaction region. The term $\tau_e [1 - e^{-t/\tau_e}]$ shows that the gain coefficient is influenced by the relaxation time τ_e when $\tau_e \gg t$, while it depends on the interaction time Δt when $t \ll \tau_e$ [33,34].

The spontaneous emission, which is the seed of the emission process, can be investigated from the quantization of the EM field. In the stored energy of the surface wave W expressed by Eq. (31), the energy of the magnetic field is not equal to that of the electric field in general, but they are almost same. The field quantization of the stored energy can be realized by introducing the photon number S such as

$$W = 2\bar{\epsilon}_{av} |\tilde{E}(t)|^2 = \hbar\omega S. \quad (78)$$

Then, the EM wave intensity is given by

$$|\tilde{E}(t)|^2 = \frac{\hbar\omega S}{2\bar{\epsilon}_{av}}. \quad (79)$$

The electron transition to a lower energy level (from b to a) corresponds the emission process and is proportional to $S + 1$. On the other hand, the electron transition to a higher energy level (from b to c) corresponds to the absorption process and is proportional to S . In the emission process consisting of stimulated and spontaneous emissions, the spontaneous emission has almost the same characteristics of the stimulated emission except that it is independent of the existing radiation field and corresponds to the zero-point energy for which $S = 1$. Using Eqs. (67) and (79) and putting $S = 1$, we get a term C_{sp} to indicate spontaneous emission by counting the electron transition from b to a and such as

$$\frac{d|\tilde{E}(t)|^2}{dt} = \left(G_{st} - \frac{1}{\tau_{rad}} \right) |\tilde{E}(t)|^2 + C_{sp}, \quad (80)$$

where

$$C_{sp} = \frac{e\bar{J}v_e\tau_e \left[1 - e^{-\frac{t}{\tau_e}}\right]}{2\bar{\epsilon}_{av}^2} \xi_m D_{spm}, \quad (81)$$

and D_{spm} is a dispersion function for the spontaneous emission and is given by

$$D_{spm} = \text{Sinc}^2\{(k_b - k_a - mG \mp \beta)\ell/2\}. \quad (82)$$

From Eq. (67), the intensity of the surface wave at the steady state is given by

$$|\tilde{E}(t)|^2 = \frac{C_{sp}}{\frac{1}{\tau_{rad}} - G_{st}}. \quad (83)$$

Then the radiation power given in Eq. (29) becomes

$$P = 2L_x L_y \sin(\theta) \sqrt{\frac{\epsilon_0}{\mu_0}} \left\{ |R^{(+)}|^2 + |R^{(-)}|^2 \right\} \frac{C_{sp}}{\frac{1}{\tau_{rad}} - G_{st}}. \quad (84)$$

When the amplification gain G_{st} is not large enough to compensate the loss to the radiation modes (i.e., $G_{st} \ll 1/\tau_{rad}$), the EM radiation will be only a spontaneous emission, and then

$$P = 2L_x L_y \sin(\theta) \sqrt{\frac{\epsilon_0}{\mu_0}} \left\{ |R^{(+)}|^2 + |R^{(-)}|^2 \right\} \tau_{rad} C_{sp}. \quad (85)$$

It is noted that the stimulated emission is difficult to be realized without setting an external cavity to reflect back the radiation field for which $1/\tau_{rad} \approx 0$.

5. Representation of the electron wavenumbers with the electron velocity

The dispersion functions D_{stm} and D_{spm} are given in terms of the electron wave numbers as shown in Eqs. (76) and (82). In this section, we rewrite these functions in more simple and practical form.

The energy of the electron at the initial state b is

$$W_b = \frac{\hbar^2 k_b^2}{2m_0} = \frac{m_0 v_b^2}{2}. \quad (86)$$

and the electron energy at the final state a is

$$W_a = \frac{\hbar^2 k_a^2}{2m_0} = \frac{m_0 v_b^2}{2} - \hbar\omega. \quad (87)$$

Then the wave number k_a is represented with the initial electron velocity v_b as

$$k_a = \frac{m_0 v_b}{\hbar} \left(1 - \frac{2\hbar\omega}{m_0 v_b^2}\right)^{1/2}. \quad (88)$$

and the difference between the initial and final wave numbers is

$$k_b - k_a = \frac{m_0 v_b}{\hbar} \left\{ 1 - \left(1 - \frac{2\hbar\omega}{m_0 v_b^2}\right)^{1/2} \right\} = \frac{\omega}{v_b} \left\{ 1 + \frac{\hbar\omega}{2m_0 v_b^2} \right\}. \quad (89)$$

For clarity, we put $v_b = v_e$ to refer to the electron velocity, then

$$\frac{(k_b - k_a - mG \mp \beta)\ell}{2} = - \left\{ (mG \pm \beta)v_e - \omega - \frac{\hbar\omega^2}{2m_0v_e^2} \right\} \frac{\ell}{2v_e}. \quad (90)$$

Similarly, the electron energy at the final state c is expressed as

$$W_c = \frac{\hbar^2 k_c^2}{2m_0} = \frac{m_0 v_b^2}{2} + \hbar\omega. \quad (91)$$

and then

$$\frac{(k_c - k_b - mG \mp \beta)\ell}{2} = - \left\{ (mG \pm \beta)v_e - \omega + \frac{\hbar\omega^2}{2m_0v_e^2} \right\} \frac{\ell}{2v_e}. \quad (92)$$

Using Eqs. (90) and (92), the dispersion function is rewritten as

$$D_{stm} = \text{Sinc}^2 \left\{ \left[(mG \pm \beta)v_e - \omega - \frac{\hbar\omega^2}{2m_0v_e^2} \right] \frac{\ell}{2v_e} \right\} - \text{Sinc}^2 \left\{ \left[(mG \pm \beta)v_e - \omega + \frac{\hbar\omega^2}{2m_0v_e^2} \right] \frac{\ell}{2v_e} \right\}. \quad (93)$$

The critical difference between $k_b - k_a$ and $k_c - k_b$ is required to obtain D_{stm} , while the difference $k_b - k_a$ is only counted to obtain D_{spm} where

$$D_{spm} = \text{Sinc}^2 \left\{ \left[(mG \pm \beta)v_e - \omega - \frac{\hbar\omega^2}{2m_0v_e^2} \right] \frac{\ell}{2v_e} \right\}. \quad (94)$$

Numerical examples of the functions D_{stm} and D_{spm} are shown in Fig. 5, where $\lambda = 0.5 \mu\text{m}$, $\Lambda = 0.4 \mu\text{m}$, $m = 3$, and $\ell = 30 \mu\text{m}$. In this example, we use the value of the coherent length of the electron wave ℓ obtained in the experiments of Refs. [27,28]. The electron velocity is $v_e \approx 1.15 \text{ m/s}$ which corresponds the acceleration voltage of $V = 37.3 \text{ kV}$.

Since the SP radiation is usually measured as a spectrum profile for fixed electron velocity v_e and radiation angle θ , we rewire the functions D_{stm} and D_{spm} as functions of measuring wavelength λ . By using Eqs. (3) and (23), the dispersion coefficient $(mG \pm \beta)v_e - \omega$ becomes

$$(mG \pm \beta)v_e - \omega = 2\pi v_e \left\{ \frac{m}{\Lambda} - \frac{1}{\lambda} \left(\frac{c}{v_e} - \cos(\theta) \right) \right\}. \quad (95)$$

We refer to the center wavelength of the emission is λ_0 , which is obtained by putting Eq. (94) equal to 1, as

$$\lambda_0 = \frac{\Lambda}{m} \left(\frac{c}{v_e} - \cos(\theta) \right). \quad (96)$$

Then, the function D_{spm} is rewritten as

$$D_{spm} = \text{Sinc}^2 \left[\frac{\pi m \ell}{\Lambda} \left(1 - \frac{\lambda_0}{\lambda} \right) \right], \quad (97)$$

and D_{stm} is rewritten as

$$D_{stm} = \text{Sinc}^2 \left\{ \pi \ell \left[\frac{m}{\Lambda} \left(1 - \frac{\lambda_0}{\lambda} \right) - \frac{hc^2}{2m_0v_e^3\lambda_0^2} \left(\frac{\lambda_0}{\lambda} \right) \right] \right\} - \text{Sinc}^2 \left\{ \pi \ell \left[\frac{m}{\Lambda} \left(1 - \frac{\lambda_0}{\lambda} \right) + \frac{hc^2}{2m_0v_e^3\lambda_0^2} \left(\frac{\lambda_0}{\lambda} \right) \right] \right\}. \quad (98)$$

where h is the Planck's constant.

Numerical examples of the dispersion functions D_{stm} and D_{spm} shown in Eqs. (97) and (98) are shown in Fig. 6. In this example, it is assumed that $\Lambda = 0.5 \mu\text{m}$, $m = 2$, $\ell = 30 \mu\text{m}$, $V = 30 \text{ kV}$, and $\theta = \pi/2$ to generate a spontaneous emission with $\lambda_0 = 0.728 \mu\text{m}$. In this example, since the emission is almost spontaneous in nature, the full width at half maximum of the spectral width

is almost 8% of the central wavelength.

It is instructive to point out that the dispersion functions D_{stm} and D_{spm} of the stimulated and spontaneous emissions are defined in terms of the so called coherent length of an electron ℓ . Due to collisions among electrons, the spreading length must not be infinitely long (i.e., shorter than the interaction length). Therefore, it should be the main cause of the spectrum broadening. In the experiments shown in Ref. [35], a grating with a $0.416 \mu\text{m}$ pitch and the electron acceleration voltage of 30 kV are used to obtain SP spontaneous radiation with a peak wavelength of $1.3 \mu\text{m}$ at the observation angle $\theta = \pi/2$. The grating length (i.e., the interaction length) is 2.5 cm. In Ref. [35], It is shown that the spectral full width at half maximum (FWHM) is $\Delta\lambda \sim 0.1 \mu\text{m}$ in the wavelength domain and is $\Delta\omega \sim 1.1 \times 10^{14} \text{ s}^{-1}$ in the angular frequency domain. It is obvious that the amounts of the broadening $(\Delta\omega)_\tau = 2\pi/\tau$ and $(\Delta\omega)_t = 2\pi/t$ due the relaxation and interaction times, respectively, are much smaller than the broadening $\Delta\omega \sim 1.1 \times 10^{14} \text{ s}^{-1}$ observed experimentally. Thus, the spectrum broadening can only be predicted by the finite length of electron spreading, which corresponds to the coherent length of the electron wave. Here, it is also very interesting to point out that $\Delta\lambda/\lambda_0 = 0.076$ in the experiment in [35] with an excellent agreement to the result shown in Fig. 6 where the spreading length of electron in the order of few tens of micrometers (i.e., $\sim 30 \mu\text{m}$). This value of the spreading length also matches with that predicted from the Cherenkov FELs experiments in [27,28].

6. Discussions and conclusions

In this section, we compare our obtained results with those given by Yariv and Shih [36] as a typical treatment for the FELs based on the longitudinal coupling configuration such as Cherenkov and SP FELs.

In Ref. [36], a periodic dielectric corrugation is used (i.e., $\sigma \approx 0$) and the authors assumed the more efficient interaction with the surface modes of the corrugation (i.e., $G_{st} \gg 1/\tau_{rad}$). Also, the inclusion of the spontaneous emission is neglected (i.e., $C_{sp} = 0$). In the nonrelativistic limit, the exchange power between the electron beam and the EM wave during the interaction time t is given by [36]

$$\Delta P_c = \frac{e\omega I t^3}{2m_0} |\tilde{E}|^2 f(\Theta), \quad (99)$$

where $I = e \int_h^{w+h} \int_{-w/2}^{w/2} (\bar{N}v_e) dx dy$ is the electron beam current and $f(\Theta)$ is the well-known dispersion function in previous theories of FELs given by

$$f(\Theta) = \frac{d}{d\Theta} \left(\frac{\sin(\frac{\Theta}{2})}{\Theta/2} \right)^2, \quad (100)$$

where $\Theta = [\beta_{eq}v_e - \omega](L_z/v_e)$ and $\beta_{eq} = (mG \pm \beta)$ in the case of the SP effect. Symbols in Eqs. (99) and (100) have the same meanings as in our present paper.

In this work, we state that the spreading length of the coherent electron wave ℓ determines the broadness profile of the dispersion function. Assuming that the collisions among electrons don't exist, ℓ could be expanded to be the full length of the interaction region L_z . This case (i.e., when $\ell \approx L_z$) represents the classical limit at which the electron is described as a point like particle moving without any perturbations from the neighboring electrons. In this limit, the dispersion function given by Eq. (93) is rewritten in terms of the classical dispersion function $f(\Theta)$ as

$$D_{stm} = \text{Sinc}^2 \left\{ \left[\frac{\Theta}{2} - \Delta\Theta \right] \right\} - \text{Sinc}^2 \left\{ \left[\frac{\Theta}{2} + \Delta\Theta \right] \right\} \approx f(\Theta) \times 2\Delta\Theta. \quad (104)$$

where $\Delta\Theta = (\hbar\omega^2/m_0v_e^2)(L_z/2v_e)$ and represents the electron recoil energy. As experiments move toward the generation of short-wavelength radiation, corrections to the classical dispersion function $f(\Theta)$ become significant. In our analysis, the quantum corrections are invoked in the effects of the electron's recoil energy and the finite length of the electron wave as shown in Eqs. (93) and (94). In the emission and absorption processes, the electron's recoil energy is $(\hbar^2\omega^2/2m_0v_e^2)$, which is quite small for most of practical cases. Then, the spreading length of the electron wave is the essential parameter in determining the gain line shape in our quantum mechanical treatment. However, if the electronic recoil is assumed to be zero, no gain is found. Approximately, the term of the electron recoil $(\hbar\omega^2/2m_0v_e^2)$ in Eqs. (93) and (94) should be considerable when $\hbar\omega/2m_0c^2 > 0.001$ (i.e., when $\lambda < 1$ nm in the x-ray range or in shorter range). From Eq. (27), the quantum corrections of the electron recoil could be essential when the electron velocity becomes very close to the speed of light in vacuum (i.e., $v_e \sim c$) and $\theta \sim 0$ where SP wavelengths will be shortest at $\theta \sim 0$. To date, the SP FEL operated in the x-ray region cannot be obtained using the current technology. This is because the SP radiation observed in the forward direction (at $\theta \sim 0$) is very weak. Another main technical restriction is that SP x-ray production requires that the electron beam must be steered extremely close to the grating (within few tens of nanometers) without striking its surface. In this paper, it is assumed that counting the electron recoil results in negligible quantum corrections to the gain in comparison with that of the spreading length of the electron wave as discussed in the end of Section 5.

Using Eq. (67) and assuming $G_{st} \gg 1/\tau_{rad}$, $C_{sp} = 0$, and $\sigma = 0$, we can write the radiation power transferred to the SP radiation ΔP after the transit time t as

$$\Delta P = G_{st}tP. \quad (105)$$

Using Eqs. (29), (77), (99), and (100), we find that the power transferred to the radiation ΔP obtained in our model is one half of with that obtained in Ref. [36] such as $\Delta P = (1/2)\Delta P_c$. It is noted that the Planck's constant shown in the denominator of Eq. (77) is canceled with that appears in Eq. (104) where $\Delta\Theta$ contains Planck's constant in the numerator. Therefore, the

quantum correction is mainly invoked in determining the dispersion relation by the coherent length of the electron wave instead of the interaction length.

We end this section by confirming that the coherent length of the electron wave should be adopted to fit the experimental spectral line of the emitted radiation. This length is influenced by the electron density of the electron beam and the initial thermal broadness of the electron velocity. However, in the ideal cases of negligible electron collisions, the coherent length might be equal to the interaction length of the device and our analytical model reduces to the classical one.

In conclusion, in our analysis of the SP radiation based on the small–signal approximation, the electron beam interacts with the surface wave of the metallic corrugation whose propagation velocity is delayed by the corrugated structure. The surface wave produces an EM radiation through the diffraction effect from the corrugated structure. The description of the surface and radiation waves is introduced basing on the Maxwell’s wave equation. We derive a generalized expression for calculating the low gain of single–pass radiation. In this expression, the profile of the gain distribution is influenced by the finite length of an electron wave and the electron’s recoil due to the emission and absorption processes. The compatibility of our analysis with already known classical analyses is confirmed.

Appendix

To take into account the statistical properties of electrons, let us assign a number ν for each electron in the electron beam. The expectation value of an arbitrary quantum mechanical operator \mathcal{R} is given by

$$\langle \mathcal{R} \rangle = \sum_{\nu} P^{(\nu)} \langle \Psi^{(\nu)}(\mathbf{r}, t) | \mathcal{R} | \Psi^{(\nu)}(\mathbf{r}, t) \rangle, \quad (A1)$$

where $P^{(\nu)}$ is the probability of finding the ν -th electron in the ensemble where

$$\sum_{\nu} P^{(\nu)} = 1. \quad (A2)$$

$|\Psi^{(\nu)}(\mathbf{r}, t)\rangle$ is the state vector of the ν -th electron and satisfies the normalization condition

$$\langle \Psi^{(\nu)}(\mathbf{r}, t) | \Psi^{(\nu)}(\mathbf{r}, t) \rangle = \int_{\mathcal{V}} |\Psi^{(\nu)}(\mathbf{r}, t)|^2 d^3r = 1. \quad (A3)$$

Also, the eigen vector $|\phi_m(\mathbf{r})\rangle$ satisfies the normalization and orthogonal conditions

$$\langle \phi_g(\mathbf{r}) | \phi_f(\mathbf{r}) \rangle = \int_{\mathcal{V}} [\phi_g(\mathbf{r})]^* \phi_f(\mathbf{r}) d^3r = \delta_{f,g}. \quad (A4)$$

Using Eq. (39), Eq. (A3), and Eq. (A4), we obtain

$$\sum_f |c_f^{(\nu)}(t)|^2 = 1. \quad (A5)$$

By substituting Eq. (39) into Eq. (A1), the expectation value of the operator \mathcal{R} is given by

$$\langle \mathcal{R} \rangle = \sum_{\nu} \sum_{g \neq f} \sum_f \left\{ P^{(\nu)} c_g^{(\nu)*}(t) c_f^{(\nu)}(t) e^{j(\omega_g - \omega_f)t} \right\} \langle \phi_g(\mathbf{r}) | \mathcal{R} | \phi_f(\mathbf{r}) \rangle. \quad (A6)$$

By defining the matrix ρ whose matrix element is given by

$$\rho_{fg}(t) = \sum_{\nu} P^{(\nu)} c_g^{(\nu)*}(t) c_f^{(\nu)}(t) e^{j(\omega_g - \omega_f)t}, \quad (A7)$$

the expectation value of \mathcal{R} can be written as

$$\langle \mathcal{R} \rangle = \sum_{g \neq f} \sum_f \rho_{fg}(t) \mathcal{R}_{gf}. \quad (A8)$$

By using Eq. (39), we rewrite Eq. (A7) in the form of

$$\rho_{fg}(t) = \left\langle \phi_g(\mathbf{r}) \left| \left\{ \sum_{\nu} |\Psi^{(\nu)}\rangle P^{(\nu)} \langle \Psi^{(\nu)}| \right\} \right| \phi_f(\mathbf{r}) \right\rangle. \quad (A9)$$

Therefore, the abstract density matrix ρ is given by

$$\rho = \sum_{\nu} |\Psi^{(\nu)}\rangle P^{(\nu)} \langle \Psi^{(\nu)}|. \quad (A10)$$

The Schrödinger equation of the eigen vector $|\Psi^{(\nu)}(r, t)\rangle$ is

$$j\hbar \frac{\partial |\Psi^{(\nu)}\rangle}{\partial t} = \left(H - j \frac{\hbar \Gamma}{2} \right) |\Psi^{(\nu)}\rangle, \quad (A11)$$

where the expectation value of the operator Γ is the electron relaxation time τ .

Using Eq. (A10) with the help of Eq. (A11), the dynamic equation of the density matrix is

$$\frac{d\rho}{dt} = \frac{1}{j\hbar} [H, \rho] - \frac{1}{2} \{(\rho - \tilde{\rho})\Gamma + \Gamma(\rho - \tilde{\rho})\}. \quad (A12)$$

The second term on the right-hand side of Eq. (A12) is a phenomenological term that represents the relaxation of electrons to their equilibrium positions.

References

- [1] S. J. Smith and E. M. Purcell, *Physical Review* **92** (1953) 1069.
- [2] K. J. Woods, J. E. Walsh, R. E. Stoner, H. G. Kirk, and R. C. Fernow, *Physical Review Letter* **74** (1995) 3808.
- [3] D. E. Wortman, R. P. Leavitt, H. Dropkin and C. A. Mossion, *Physical Review A* **24** (1981) 1150.
- [4] M. Goldstein, J. E. Walsh, M. F. Kimmitt, J. Urata, and C. L. Platt, *Applied Physics Letter* **71** (1997) 452.
- [5] E. J. Burdette and G. Hughes, *Physical Review A* **14** (1976) 1766.
- [6] G. Doucas, J. H. Mulvey, M. Omori, J. Walsh and M.F. Kimmitt, *Physical Review Letter* **69** (1992) 1761.
- [7] J. Urata, M. Goldstein, M. F. Kimmitt, A. Naumov, C. Platt, and J. E. Walsh, *Physical Review Letter* **80** (1998) 516.
- [8] H. L. Andrews, C. A. Brau, and J. D. Jarvis, C. F. Guertin, A. O'Donnell, B. Durant, T. H. Lowel, and M. R. Mross, *Physical Review Special Topics - Accelerators and Beams* **12** (2009) 080703.
- [9] A. Bakhtyari, J. E. Walsh, and J. H. Brownell, *Physical Review E* **65** (2002) 066503.
- [10] A. S. Kesar, R. A. Marsh, and R. J. Temkin, *Physical Review Special Topics–Accelerators and Beams* **9** (2006) 022801.
- [11] K. Ishi, Y. Shibata, T. Takahashi, S. Hasebe, M. Ikezawa, K. Takami, T. Matsuyama, K. Kobayashi, and Y. Fujita, *Physical Review E* **51** (1997) R5212(R).
- [12] G. Kube, H. Backe, H. Euteneuer, A. Grendel, F. Hagenbuck, H. Hartmann, K. H. Kaiser, W. Lauth, H. Schöpe, G. Wagner, Th. Walcher, and M. Kretzschmar, *Physical Review E* **65** (2002) 056501.
- [13] V. L. Bratman, A. E. Fedotov, and P. B. Makhalov, *Applied Physics Letter* **98** (2011) 061503.
- [14] Y-M. Shin, J-K. So, K-H Jang, J-H. Won, A. Srivastava, and G-S. Park, *Applied Physics Letter* **90** (2007) 031502.
- [15] J. M. Wachtel, *Journal of Applied Physics* **50** (1979) 49.
- [16] L. Schächter and A. Ron, *Physical Review A* **40** (1989) 876.
- [17] K. J. Kim and S. B. Song, *Nuclear Instruments and Methods in Physics A* **445** (2000) 276.
- [18] H. L. Andrews, C. H. Boulware, C. A. Brau, and J. D. Jarvis, *Physical Review Special*

- Topics–Accelerators and Beams **8** (2005) 050703.
- [19] G. F. Mkrtchian, *Physical Review Special Topics - Accelerators and Beams* **10** (2007) 080701.
- [20] A. Friedman, A. Gover, G. Kurizki, S. Ruschin, and A. Yariv, *Reviews of Modern Physics* **60** (1988) 471.
- [21] J. D. Jarvis, H. L. Andrews, and C. A. Brau, *Physical Review Special Topics–Accelerators and Beams* **13** (2010) 020701
- [22] D. Li, M. Hangyo, Y. Tsunawaki, Z. Yang, Y. Wei, S. Miyamoto, M. R. Asakawa, and K. Imasaki, *Applied Physics Letter* **100** (2012) 191101.
- [23] M. Yamada, *IEEE Journal of Quantum Electronics* **35** (1999) 147.
- [24] H. Fares and M. Yamada, *Nuclear Instruments and Methods in Physics A* **659** (2011) 519.
- [25] M. Yamada and H. Fares, *Nuclear Instruments and Methods in Physics A* **709** (2013) 108.
- [26] H. Fares, M. Yamada, and K. Ohmi, *IEEE Journal of Quantum Electronics* **49** (2013) 970.
- [27] Y. Kuwamura, M. Yamada, R. Okamoto, T. Kanai, and H. Fares, *Journal of Applied Physics* **104** (2008) 103105.
- [28] H. Fares, M. Yamada, Y. Kuwamura, I. Matsumoto, and T. Kanai, *IEEE Journal of Quantum Electronics* **46** (2010) 981.
- [29] V. P. Stukhatme and P. A. Wolff, *Journal of Applied Physics* **44** (1973) 2331.
- [30] D. Marcuse, *Principles of Quantum Electronics*, (Academic Press, New York, 1980), ch. 7.
- [31] H. Fares, *Nuclear Instruments and Methods in Physics A* **773** (2015) 151.
- [32] L. Schächter, *Beam-Wave Interaction in Periodic and Quasi-Periodic Structures*, (Springer-Verlag Berlin Heidelberg, 2011), p. 234
- [33] H. Fares, M. Yamada and Y. Kuwamura, *Japanese Journal of Applied Physics* **49** (2010) 096402.
- [34] H. Fares and M. Yamada, *Physics of Plasmas* **18** (2011) 093106.
- [35] Y. Neo, H. Shimawaki, T. Matsumoto, and H. Mimura, *Journal of Vacuum Science & Technology B* **24** (2006) 924.
- [36] A. Yariv and C. C. Shih, *Optics Communications* **24** (1978) 233.

Figures

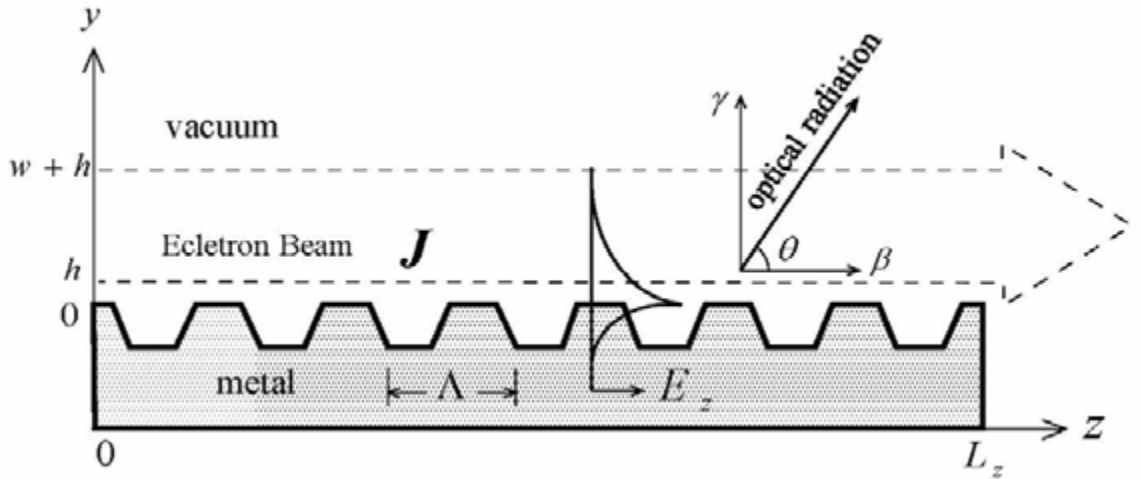


Fig.1. The configuration of the Smith–Purcell FEL. The electron beam moves above the grating surface in the z direction. The grooves repeat periodically with the grating period Λ , the grating surface at $y = 0$, and the system is invariant in the x direction.

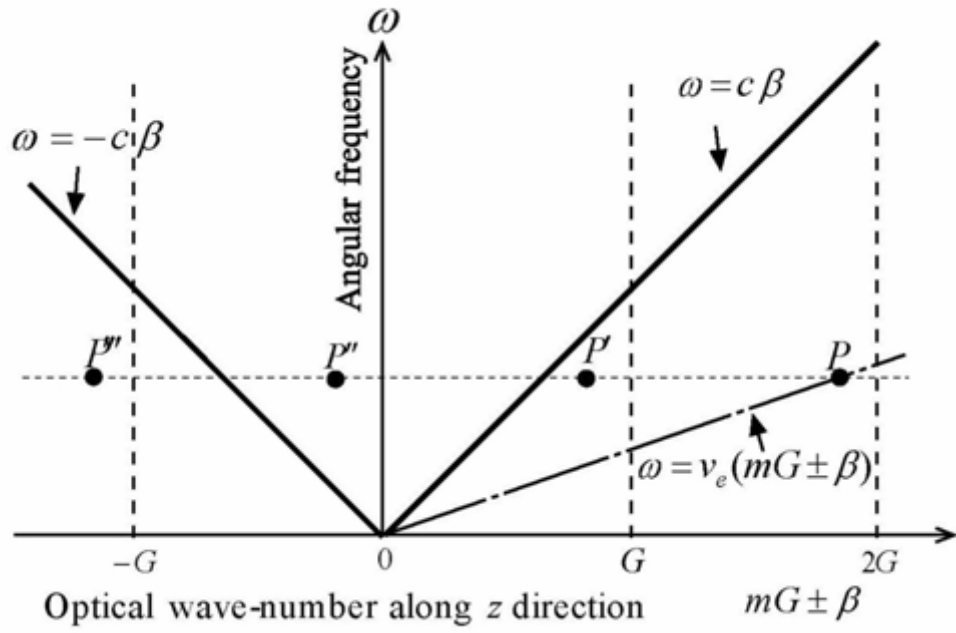


Fig.2 Relation between the angular frequency and the EM wave-number along z direction. When the EM field interacts with the electron beam at point P located at the beam line $\omega = (mG \pm \beta)v_e$, radiation is generated at point P'' located between the light lines $\omega = \pm c\beta$.

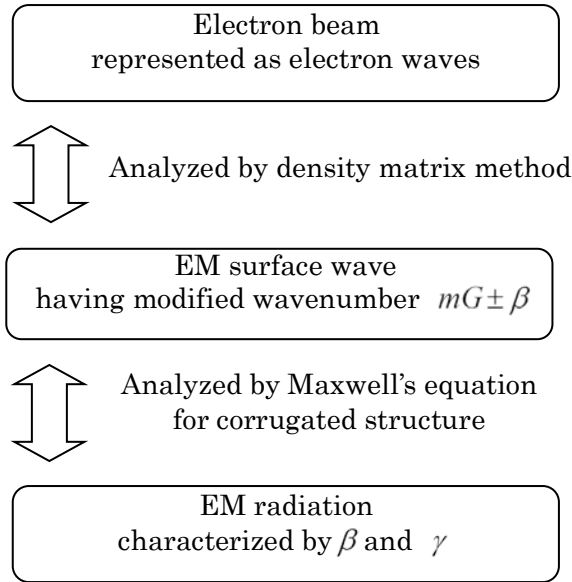


Fig.3. Illustration of the analytical model used in this work. Electron beam excites EM surface wave on the corrugation having field components with wavenumbers $mG \pm \beta$. This interaction is analyzed basing on the density matrix method. The interacted surface field couples to one of radiation modes, and then radiation is generated. This coupling is analyzed by the Maxwell's wave equation.

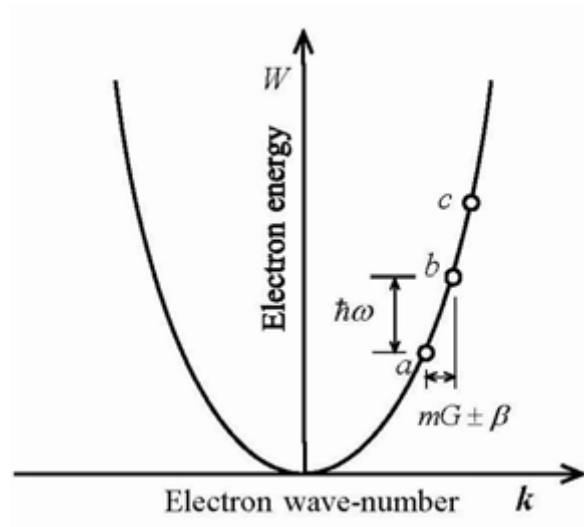


Fig.4 Energy diagram of a traveling electron in vacuum.

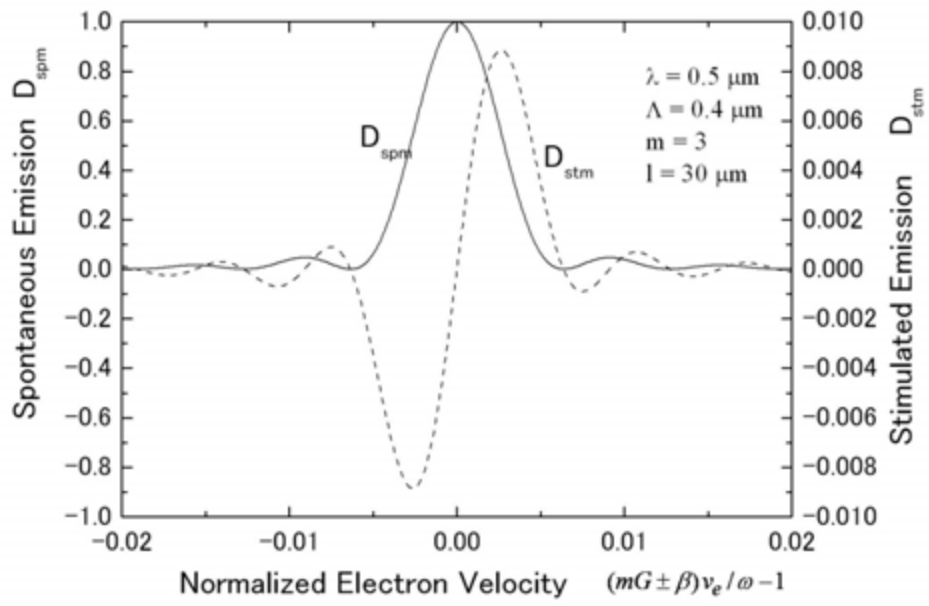


Fig. 5. A numerical example showing the dispersion functions D_{stm} and D_{spm} as function of the electron velocity.

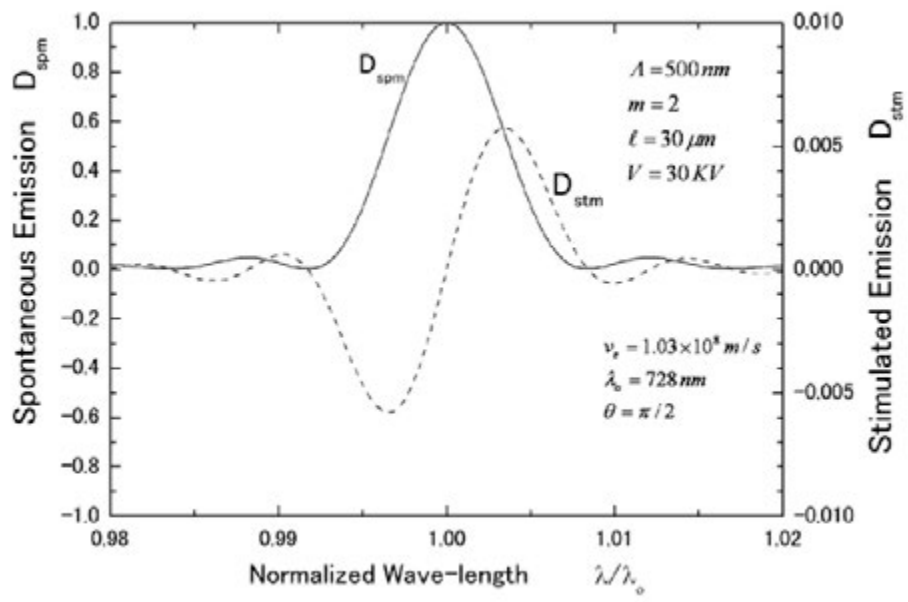


Fig. 6. A numerical example showing the dispersion functions D_{stm} and D_{spm} as function of the optical wavelength.